

Design of Performance Characteristics on Laser Treated Denim Fabric

Nele MANDRE^{1*}, Tiia PLAMUS¹, Angelika LINDER¹, Toivo VARJAS², Jüri MAJAK³,
Andres KRUMME¹

¹Department of Material and Environmental Technology, Laboratory of Polymers and Textile Technology, Tallinn University of Technology, Ehitajate tee 5, 12616, Tallinn, Estonia

²Department of Electrical Power Engineering and Mechatronics, Laboratory of Lightning Technology, Tallinn University of Technology, Ehitajate tee 5, 12616, Tallinn, Estonia

³Department of Mechanical and Industrial Engineering, Tallinn University of Technology, Ehitajate tee 5, 12616, Tallinn, Estonia

<https://doi.org/10.5755/j02.ms.33259>

Received 26 January 2023; accepted 16 May 2023

The current paper covers an experimental study, mathematical modelling, and design optimization of the laser treatment process of denim fabrics. Laser fading is used in the finishing phase of garment production, unfortunately, it decreases fabric durability. Denim fabric is known as a cotton fabric but nowadays it is blended with other fibres to improve fabric properties. For this reason, the main purpose of this study was to test multicomponent fabric longevity after laser treatment. The knowledge from this study is used by garment production company. The tear force, abrasion resistance, and colour difference are considered as performance characteristics of laser treated denim fabrics subjected to maximization. To achieve the goals, novel, mathematical models were developed. In the preliminary tests, the design space was determined. The full factorial design of experiments was utilized in the experimental study and the values of the performance characteristics are measured. Based on the results of the experimental study the artificial neural network and Haar wavelet based mathematical models were developed to predict the behaviour of the tear force, abrasion resistance, and colour difference. The artificial intelligence-based multicriteria design optimization procedure is developed.

Keywords: laser treated denim fabrics, artificial neural network, multicriteria optimization, wavelet method.

1. INTRODUCTION

Denim fabric finishing is the final process of garment production performed on garment, fabric or yarn to give a fashionable desired appearance to the customer. Denim finishes can be divided into mechanical and chemical. Mechanical processes, are for example, stone washing, sandblasting, machine or hand sanding. The most commonly used chemical washes are bleaching, acid, and enzyme washing. Usually, pumice stones are used in stone washing where about 1 kg of stones are needed for the treatment of 1 kg of denim fabric. Thus, this process produces large amounts of sludge in the water that needs to be filtered. Bleaching is considered a harmful chemical process to human health. Based on previous studies it can cause damage to cotton and corrosion to a washing machine [1–3].

According to previous studies, good fitting, comfortable denim jeans with attractive design are important characteristics for customers. In addition, consumer awareness of the negative impact of the textile industry on the environment has led them to more sustainable thinking and choosing clothes that last longer. Manufacturers use different techniques to improve the textile production process and extend the physical longevity of clothing by reducing the waste. A laser technology is an innovative sustainable alternative to common finishing methods for the treatment of denim garments [4–8]. Laser

is an optical device developed to produce intense and coherent beam of light. Laser beams applied on a fabric surface in the textile industry provide different applications; they are used for engraving, laser welding, laser bonding, and controlled cutting. Spanish company Jeanologia has developed a sustainable laser technology for fading denim fabrics to obtain a special appearance and reduce the use of water, harmful chemicals, and save energy. In addition, it is a more accurate and flexible method than other mentioned methods with high productivity. Also, laser technology helps to reduce time, work, and resource consumption. CO₂ laser with the wave length of 10 μm is the most widely used laser in the textile industry because of high efficiency. Based on Muthu and Gardetti [9], Gandhi [10], Angelova *et al.* [11], Vilumsonė-Neme [12], Juciene *et al.* [13] the laser speed, the laser power, and energy density of laser beam have the greatest impact on fabric properties. For example, Juciene *et al.* [13] determined the impact of laser treatment and industrial washing on the tensile properties of denim fabrics. The fabric was made of 98 % cotton and 2 % elastane. Test results showed that laser treatment and industrial washing increased fabric thickness but decreased mass per unit area and breaking force. It was also noticed in Juciene, that weft yarns were less damaged by the laser beam because warp yarns are more dominant on the surface of the fabric [13].

Kan [14] proved the effectiveness of laser technology. Two laser-treated cotton denim fabrics were prepared. One

* Corresponding author. Tel.: +372 55562824.
E-mail: nele.mandre@taltech.ee (N. Mandre)

was manufactured with low-twist yarn spun by torque-free ring-spinning technology, and the other was manufactured with conventional ring-spun yarn. After CO₂ laser treatment colour fastness and dimensional stability of both fabrics were compared with the conventional cellulase treatment. Kan found that laser beam is able to generate a faded look on denim garment within 3 min at room temperature while the stone washing process with enzyme generates the same design for 45 min at 55 °C. Thus, laser technology saves energy, time, and water [14].

Many previous studies have compared laser technology with conventional washing processes. Ozguney *et al.* [15] examined the effect of a CO₂ laser beam on denim fabric tensile and tear properties. Also, abrasion resistance, the static and kinematic friction coefficient, and optimum process conditions were determined. They concluded that a laser beam decreased fabric tear and tensile strength as well as abrasion resistance. Although changes in the warp and weft direction were different, the laser faded process increased the static and dynamic friction coefficients. Dalbaşı *et al.* [16] compared unwashed and washed laser treated 100 % cotton denim fabrics. Their results showed that the number of washing cycles did not affect the tensile and tear properties significantly, but the laser process affected all the tested fabrics' warp and weft yarn strength properties negatively. Washing cycles and laser process decreased the abrasion resistance of the tested fabrics. In Solman and Saha's [17] research laser fading, hand sand brushing, and potassium permanganate spraying were applied on denim fabric for fading. After testing, the mechanical and aesthetic properties of the fabric were compared with untreated denim. As a result, hand sand brushed fading had the highest negative impact on fabric tear and tensile properties.

Studies on cotton blended with elastane are scarce. No research into the properties of the fabrics containing multicomponent yarns in the core of weft yarn has been reported. Although the multicomponent fabric is widely used in garment production. In addition, knowledge acquired from this study is used by garment producer company. The main purpose of blending fibres is to improve fabric performance properties. Blending different fibres into one yarn helps to compensate one fibre weaknesses or disadvantages. In the current study, 3/1 twill weave fabric was made that consisted of four different fibres to provide comfortable and durable clothing. Abrasion resistance and tear force are considered as durability properties in the current study. Abrasion resistance is the ability of a fabric surface to withstand abrasive stresses. Tear force is the force to begin or continue a tear in a fabric under specified conditions. According to Hutten [18] under tearing load one or at most a few yarns share the load. Denim fabric warp yarn was made of cotton fibre. But the weft yarn core part was ternary, containing elastane, viscose, and polyester covered with cotton. Cotton is a strong but rigid fibre because of its crystalline structure. Polyester-cotton blend was used to improve cotton durability properties. Polyester has higher abrasion resistance and crease recovery properties than cotton. Elastane was blended with cotton to add elasticity and improve the stretchability of denim fabric by providing comfort to the wearer [10, 19]. Viscose is a regenerated fibre made from renewable material cellulose,

which makes it a sustainable alternative to cotton. Cotton and viscose have different crystallinity, which also influences fibre properties [20].

The HWM was proposed originally by Chen and Hsiao in 1997 for solving ordinary differential equations [21]. The wavelet expansion introduced in [21] has been utilized by many of authors for function approximation (monograph [22], papers [23–25], etc.). The higher order Haar wavelet method (HOHWM) was introduced recently by Majak *et al.* as an improvement of HWM [26]. Utilizing the HOHWM based wavelet expansion approach enables to achieve principal improvement of the absolute error and the rate of convergence in comparison with the widely used HWM (see [27–32] for differential equations and [33, 34] for function approximation).

A feedforward artificial neural network is the simplest ANN in which the nodes do not form a cycle [35]. After Rosenblatt perceptron was developed in the 1950s, there was a lack of interest in neural networks for several decades until the backpropagation algorithms for training a multilayer neural network were implemented in parallel by several researchers [36]. Despite its simplicity feedforward ANN forms a powerful tool for function approximation due to its hierarchical structure. The accuracy and configuration of the ANN are studied in detail in [37]. The current work group has long time experience with the adaption of feedforward ANN for a wide range of engineering applications covering the design of composite laminates with structural health monitoring capabilities [38], the design of car frontal protection systems [39], modelling and design of large composite parts [40], modelling reprocessing of the glass fiber reinforced plastic scrap [41], etc.

The mathematical models developed were utilized for evaluations of objective functions. The optimization was performed by applying a multicriteria genetic algorithm (GA). GA was introduced by J.H. Holland in 1992 and is currently well-known and one of the most widely used methods in engineering optimization [42]. The main advantages of the GA over traditional gradient based methods are capabilities to handle integer and discrete variables and avoid local extremes [42]. As it is common for population based evolutionary algorithms, GA does not require that the objective and constraint functions are differentiable. The elitist nondominated sorting based multiobjective genetic algorithm NSGA-II was developed by Deb *et al.* in 2002 [43]. GA together with ANN found wide use in design optimization of composite structures [44–47]. In [44] the neural network and the random forest are utilized for determining the delamination of an arbitrary length at a random point of a uniform composite beam using modal properties. In [45] single and multiobjective design is utilized for determining optimal stacking sequences of dimensionally stable symmetric balanced laminated carbon/epoxy composites. In [46] the optimization methodology has been proposed to solve design pultrusion processes for industrial applications employing the design of experiments and the response surface techniques.

The current work group has utilized GA with success for solving a wide class of engineering design problems including the design of composite laminates with structural health monitoring capabilities [38], the design of car frontal

protection systems [39], multi-criteria optimization of large composite parts [40], 3D optimal material orientation problems [48], etc.

The main aim of the current study is to find optimal power and the laser cutter head speed values that have a minor effect on denim fabric durability properties. In this study, laser treated denim properties are compared with the properties of raw denim. To determine the damage to the fabric structure due to the laser fading process, the tear strength and abrasion resistance of the fabrics were measured. In addition, colour coordinates were measured to estimate the damage to the fabric as well as the visual effect. Based on the workgroup long-time experience in the area of engineering optimization and the above-mentioned simultaneous goals, the multicriteria optimization problem was formulated and solved by utilizing modern artificial intelligence tools.

In this work, two recent mathematical models were developed for modelling the objective functions: Haar wavelet based model and the feedforward artificial neural network (ANN) model. The deterministic Haar wavelet method (HWM) can be utilized in the case of a limited dataset and the stochastic ANN model in the case of a complete dataset.

2. MATERIALS AND METHODS

2.1. Materials

In this study, 3/1 Z twill weave denim fabric was prepared by the Turkish company Kipaş Holding. Fabric warp yarn was made of cotton; the weft yarn core part contained polyester, viscose, and elastane, covered with cotton yarn. Table 1 gives an overview of the structural properties of the used denim fabric.

Table 1. Structural properties of the denim fabric

Construction		Yarn count, Ne*		No of threads, per/cm		Mass per unit area, g/m ²	Fibre composition, %
		warp	weft	warp	weft		
Denim fabric	3/1 twill weave	13.1/1	18/1	44	22	330	69 % cotton (CO); 19 % polyester (PES); 10 % viscose (CV) 2% elastane (EL)

*Ne (English cotton count) Number of hanks of 840 yards (yd) of yarn weighing 1 lb. (1yd = 0.91 m; 1 lb = 0.45 kg)

2.2. Methods

The fabric was faded by using LMP9001300 PIRANHA X carbon dioxide (CO₂) laser with a wavelength of 10.6 µm. Laser lens focal distance, i.e. the distance from the lens to the point at which the laser beam converges, was 8 mm. Laser spot radius was 0.1 mm. Laser specification is shown in Table 2. Different powers and the speed of the laser cutter head were applied to the denim fabric to determine the effect of a laser beam on the physical properties of the fabric. The preliminary tests were performed to determine the design space. Based on the

authors' previous experience different laser cutter parameters were tested: the speed of the laser cutter head was between 100 to 500 mm/s and power between 11 to 20 W.

Table 2. Specifications of the laser fading machine

Manufacturer model	LMP9001300 PIRANHA X
Laser medium	CO ₂
Wavelength	10.6 µm
Maximum laser power	100 W
Maximum speed of the laser cutter head	60 000 mm/min
Laser spot radius	0.1 mm
Energy density with the power of 14 W	446 W/mm ²
Energy density with the power of 16 W	509 W/mm ²

The beam speed lower than 230 mm/s and power higher than 18 W resulted in very strong fading that broke the fabric. The speed of the laser cutter head after 350 mm/s and laser beam power lower than 11 W gave no visually visible faded appearance to the fabric for this reason, laser power for physico-mechanical tests was chosen 14, 16 and 18 W and the speed of the laser cutter head 230, 270, 310, 350 mm/s. The full factorial design of the experiment was performed with five levels for laser power (14, 15, 16, 17, 18 W) and four levels for the speed of the laser cutter head (230, 270, 310, 350 mm/s). Thunder Laser RDworks V8 software was used to set the speed and power parameters.

ISO standard EN ISO 12947-2:2016 Textiles – determination of the abrasion resistance of fabrics by the Martindale method – Part 2: Determination of specimen breakdown was used to test the abrasion resistance of the laser treated fabric. Three test specimens with a diameter of 38 mm were cut from each combination of the laser treated fabric. Martindale abrasion tester James Heal 1605 was used to test the abrasion resistance. Martindale polyurethane foam (with a diameter of 38 mm), Martindale abrasion cloth SM25 (with a diameter of 140 mm) and woven felt (with a diameter of 140 mm) were used as auxiliary materials. The number of rubs was set until two yarns were broken (ISO 12947-2:2016). Damaged and broken yarns were examined using Dino-Lite Digital Microscope AM4113T [49].

Tear force tests were performed following the standard EN ISO 13937-2:2000 Textiles – Tear properties of fabrics – Part 2: Determination of tear force of trouser-shaped test specimens (Single tear method). Tear force tests were carried out using Instron 5866 tensile testing machine and Bluehill software. Five test specimens with the dimensions 200 mm in length and 50 mm in width were cut along the warp and five along the weft direction of laser treated fabrics. A longitudinal slit of 100 mm was cut in the centre of the test specimen. The end of the tear was marked 25 mm from the uncut end of the specimen. A load cell with a maximum capacity of 500 N was used for the tear force tests, the gauge length was set to 100 mm and pulled apart at a rate of 100 mm/min. An average tear force in Newtons (N) was calculated [50].

CIE2000 colour-difference formula was used to measure denim fabrics colour difference after laser treatment. A formula was developed to improve the correlation between the visual degree of colour difference

and the numerical values. The colour change of laser treated denim fabrics was measured by 3NH Technology spectrophotometer YS33060. Tested fabrics L^*, a^*, b^* parameters were measured to calculate the surface colour change ΔE_{00} . In MacDougall (2002) the following formulas were utilized to calculate ΔE_{00} [51]:

$$\Delta E_{00} = \sqrt{\left(\frac{\Delta L^*}{k_L S_L}\right)^2 + \left(\frac{\Delta C^*}{k_C S_C}\right)^2 + \left(\frac{\Delta H^*}{k_H S_H}\right)^2 + \left(R_T \left(\frac{\Delta C^*}{k_C S_C}\right) \left(\frac{\Delta H^*}{k_H S_H}\right)\right)^2}, \quad (1)$$

where

$$L' = L^*; a' = a^*(1 + G); G = 0.5 \left(1 - \frac{\bar{c}_{ab}^*}{\bar{c}_{ab}^* + 25^2}\right)$$

$$b' = b^*; C' = \sqrt{(a')^2 + (b')^2}; h' = \tan^{-1}\left(\frac{b'}{a'}\right);$$

C^* is the Munsell Chroma that indicates saturates; H^* is the Munsell Hue that indicates hue; S_L, S_C, S_H are weighing coefficients and k_L, k_C, k_H are parametric coefficients; L^* indicates the lightness (white-black); a^* , (red-green) and b^* (yellow-blue) are the chromaticity coordinates, where $+a^*$ shows the fabric redness, and $-a^*$ is green direction; $+b^*$ is the yellow direction; $-b^*$ is the blue direction; ΔL^* is the lightness difference; ΔC^* is the saturation difference; ΔH^* is the Hue difference.

2.3 Mathematical modelling

In the following, the mathematical models are developed for modelling the laser treatment process of denim fabrics. The treatment parameters, laser power and the speed of the laser cutter head are considered as design variables. Based on our experimental study, the mathematical models were developed for describing the behaviour of the tear and weft strength, abrasion resistance and colour difference.

2.3.1. ANN based function approximation models

The ANN provides powerful tools for function approximation due to its hierarchical structure. The feedforward ANN model with one hidden layer was utilized. The nonlinear sigmoid and linear activation functions were used in hidden and output layers, respectively. The initial number of neurons in the hidden layer N_h was specified as [37, 53].

$$N_h = \frac{(N_{in} + \sqrt{N_{tr}})}{L}, \quad (2)$$

where L is the number of hidden layers, N_{in} and N_{tr} stand for the number of inputs and capacity of the training dataset, respectively.

The normalization is suggested for the ANN model development and is necessary for further optimization. The accuracy of the ANN model is estimated using the mean square error (Fig. 10). The normalized functions are non-dimensional and remain in the same range. The normalization of the design variables is performed as:

$$X = \frac{x - x_{min}}{x_{max} - x_{min}}, \quad Y = \frac{y - y_{min}}{y_{max} - y_{min}};$$

$$x_{min} = 14, \quad x_{max} = 18, \quad y_{min} = 230, \quad y_{max} = 350. \quad (3)$$

where x and y stand for the laser power and the speed of the laser cutter head, respectively. The normalized variables are denoted by capital letters. Keeping in mind further optimization, the functions are normalized as

$$F_{SWarp}(X, Y) = \frac{f_{SWarpMax} - f_{SW}(x, y)}{f_{SWarpMax} - f_{SWarpMin}};$$

$$F_{SWeft}(X, Y) = \frac{f_{SWeftMax} - f_{SW}(x, y)}{f_{SWeftMax} - f_{SWeftMin}}. \quad (4)$$

$$F_{CDiff}(X, Y) = \frac{f_{CDiffMax} - f_{SW}(x, y)}{f_{CDiffMax} - f_{CDiffMin}};$$

$$F_{AResist}(X, Y) = \frac{f_{AResistMax} - f_{SW}(x, y)}{f_{AResistMax} - f_{AResistMin}}. \quad (5)$$

In Eq. 3 the indexes *max* and *min* refers to the estimated maximum and minimum values of the functions obtained from experimental data. The accuracy of the ANN model developed to show the colour difference is satisfactory. However, the results (i.e., models and also MSEs) obtained in repetitive runs may vary remarkably, especially in the case of tear force models, where the dataset is even smaller (12 points). For this reason, in the following the ANN model has been left in reserve for use with a complete dataset. Instead, recent but simple Haar wavelet based deterministic function approximation techniques are utilized for preliminary design with a limited dataset.

2.3.2. Haar wavelets based function approximation models

The Haar wavelet based function approximation approach used herein is based on HOHWM expansion introduced by authors in [26]. The 2D function can be expanded into Haar wavelets as

$$\frac{\partial^{p+q} f}{\partial x^p \partial y^q}(x, y) = \sum_{i=1}^{2^M} \sum_{j=1}^{2^M} a_{ij} h_i(x) h_j(y), \quad (6)$$

where

$$h_i(x) = \begin{cases} 1 & \text{for } x \in [\xi_1(i), \xi_2(i)] \\ -1 & \text{for } x \in [\xi_2(i), \xi_3(i)] \\ 0 & \text{elsewhere} \end{cases}, \quad (7)$$

and

$$\xi_1(i) = A + 2(k+1)\mu\Delta x,$$

$$\xi_2(i) = A + 2(k+1)\mu\Delta x,$$

$$\xi_3(i) = A + 2(k+1)\mu\Delta x,$$

$$\mu = \frac{M}{m}, \quad \Delta x = \frac{B-A}{2^M}, \quad M = 2^J. \quad (8)$$

The Haar functions $h_i(x)$ and $h_j(y)$ defined by Eq. 7 represent the square waves [30]. The parameters p and q in Eq. 6 stand for the order of derivatives, with respect to the coordinates x and y , respectively. In Eq. 5 $m = 2^J$ is a resolution parameter with a maximum value $M = 2^J$ and k is the translation parameter. The coefficients a_{ij} in Eq. 6 can be determined by satisfying the $p + q$ -th order integral of Eq. 6 in collocation points. In the case of the uniform grid and collocation points located in the centre of “elements”, we obtain

$$x_l = \frac{(l-0.5)}{2M}, y_r = \frac{(r-0.5)}{2M}, l, r = 1, 2, \dots, 2M. \quad (9)$$

In the cases where the behavior of the function is critical near boundary, the Chebyshev-Gauss-Lobatto grid can be utilized. The higher order Haar wavelet based function approximation was introduced in 2018 and the results of analytical convergence are not yet available. However, based on the numerical convergence analysis studied in [27–32], it can be expected that the values of the method parameters $p = q = 1$ and $p = q = 2$, lead to the second and fourth order convergence, respectively. Direct function approximation with Haar wavelets, i.e., case $p = q = 0$ provides just first order convergence [33, 34]. Note that increasing the values of the parameters of the method will increase the complexity of implementation since the complementary $n + m$ constants/functions of the integration need to be determined. However, the increase in complexity is not substantial for $p, q \leq 2$. The numerical convergence analysis is performed on theoretical samples where the mesh can be simply varied and the exact analytical solution is known. As a rule, the higher values p and q provide higher accuracy in the case of fixed minimum mesh size [33, 34]. The response surfaces developed by Haar wavelet based function approximation models are given in the results section.

2.4. Multicriteria design optimization

In the following, the multicriteria design optimization (MDO) is performed considering tear and weft strengths, abrasion resistance and colour difference as objective functions. Note that in the case of all four objectives considered, a higher value is preferred. However, the normalized objectives (Eq. 5 and Eq. 6) are subjected to minimization, i.e.:

$$F = [F_{SWarp}(X, Y), F_{SWeft}(X, Y), F_{CDiff}(X, Y), F_{AResist}(X, Y)] \rightarrow \min, \quad (10)$$

where X and Y stand for the nondimensional design variables (laser power and the speed of the laser cutter head) given by Eq. 4. Based on the preliminary analysis of the objective functions the weighted summation technique and the Pareto concept are utilized. The pairwise analysis of the objectives performed shows that the tear and weft strengths are not contradictory, but both are contradictory with the colour difference function. Thus, the tear and weft strengths as non-conflicting criteria are combined using the weighted summation technique:

$$F_{Strength} = w_1 * F_{SWarp}(X, Y) + w_2 * F_{SWeft}(X, Y); \quad (11)$$

$$w_1 + w_2 = 1, \quad (12)$$

where w_1 and w_2 stand for the weights (importance) of the criteria. Detailed description of the application of optimization techniques is given in results section 3.4.

3. RESULTS

Based on the mathematical models, the multicriteria optimization problem is formulated and solved. As a result, the optimal values of the laser treating parameters and objective functions are determined.

3.1. Tear force

The response surface of tear force in warp and weft directions is depicted in Fig. 1. It can be observed from Fig. 1, that in warp directions, at increasing the laser beam power, the resistance to tear decreases.

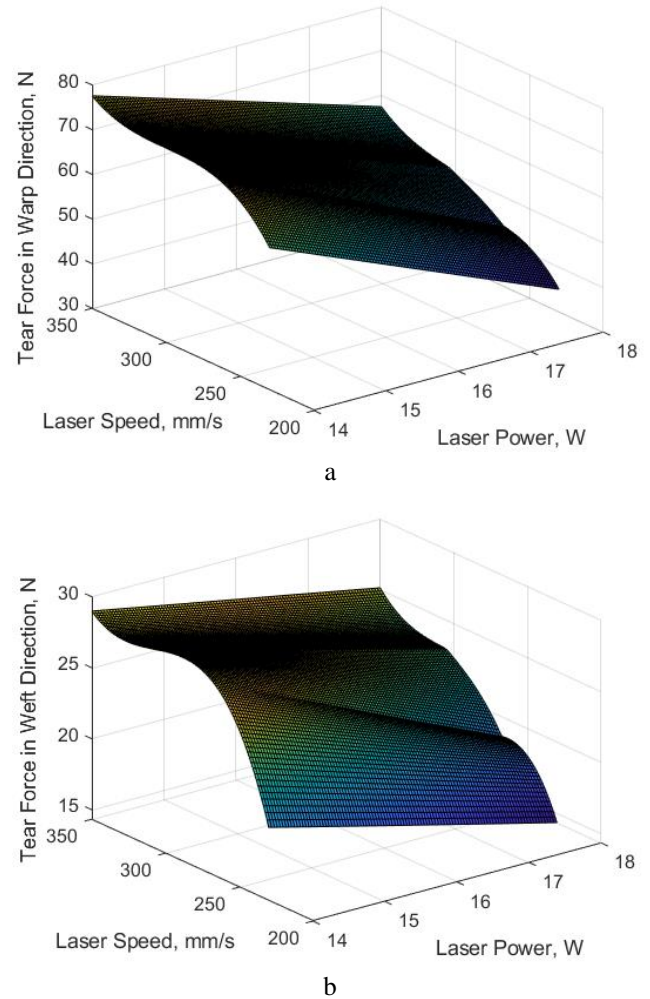


Fig. 1. Response surfaces of tear force: a – warp direction; b – weft direction

Fabrics that were treated with the laser power of 14 W showed higher resistance to tear between (62–76) N. But the tear force values of the fabrics that were treated with the power of 16 W were between (33–55) N in the warp direction. Thus, the tear force was reduced by approximately half (45 %). Fabrics that were treated with the laser power of 18 W could not withstand the tearing and these tests failed in the warp direction. In twill construction, warp yarns are more predominant on the fabric surface. Laser beam burned warp yarns of denim fabric more intensively and it caused significant difference in tear force value between warp and weft yarns. Thus, during the tearing process, warp yarns could not tear weft yarns and ruptured.

All the tested warp yarns of fabrics were made of cotton. Thus, the strength differences were influenced by the weft yarn strength. In weft directions with a power of 14 W laser treated fabrics, tear forces were more than 40 N and with the power of 16 W tear forces were approximately (20–30) N lower than in the warp direction. Tear force values of 18 W laser treated fabrics were very low, between

(1–7) N.

Increasing the speed of the laser cutter head, the tear force also increased (Fig. 2). Fabric treated with parameters of 14 W and 230 mm/s showed the tear force (62 ± 9) N and with the speed of the laser cutter head of 350 mm/s the force was (76 ± 6) N in the warp direction. The difference was 14.1 N, which means that the speed decreased the tear force of the denim fabric by 19 %. At the laser beam with the power of 16 W and the lowest speed of the laser cutter head 230 mm/s the tear force was (33 ± 2) N and with the same power but at the highest speed 350 mm/s, the force was (55 ± 4) N. The speed decreased the tear force by 39 %.

The laser beam with the power of 14 W and the speed of the laser cutter head of 350 mm/s decreased the fabric force only by 13.6 % in the warp and 15.5 % in the weft direction as compared with the raw denim fabric. The standard deviation ratio was quite high (standard deviation 6 in the warp and 1 in the weft direction). The reason might be the uneven laser fading throughout the fabric.

According to the test results, laser power beam 16 W appeared most suitable for fading of denim fabric with the speed of the laser cutter head of 350 mm/s. And laser power 14 W is suitable to use with a lower speed of the laser cutter (230 mm/s) to satisfy optimum durability and provide a visually visible fading appearance.

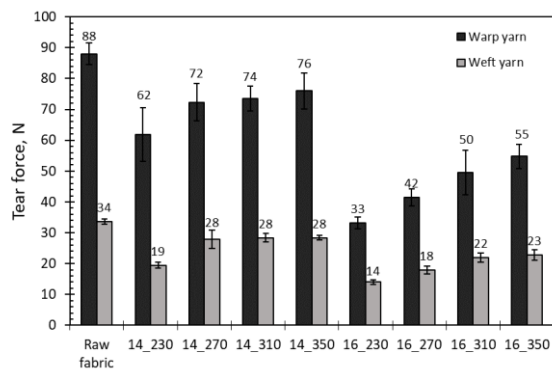


Fig. 2. Comparison of tear force of laser faded denim fabrics

3.2. Abrasion resistance

Laser treatment with different speed of the laser cutter head and power combinations affected the tested fabrics' resistance to abrasion significantly. All the tested fabrics treated with the power of 14 W showed abrasion resistance of 25 000 rubs (Fig. 4). Thus, the speed did not influence denim fabrics' resistance to abrasion. Laser power of 14 W decreased laser treated fabrics' abrasion resistance by approximately 17 % as compared with untreated denim fabrics. Denim fabrics treated with laser power of 16 W and the speed of the laser cutter head of 230 mm/s showed abrasion resistance of 14 000 rubs. By increasing the speed up to 350 mm/s, the resistance to abrasion increased to 11 000 rubs, from 14 000 rubs to 25 000 rubs. Thus, the abrasion resistance of fabric laser treated with the power of 16 W and the speed 350 mm/s was the same as that of fabrics treated with the power of 14 W. The power of 16 W and the slowest speed of the laser cutter head 230 mm/s decreased the abrasion resistance of the fabric by 53 % as compared with the untreated denim fabric. At the power of 18 W and the lowest speed of 230 mm/s, the abrasion

resistance of the laser treated fabric was only 1000 rubs. Thus, the abrasion resistance was decreased by approximately 97 % as compared with an untreated denim fabric. Denim fabric treated with the power of 18 W and the speed of the laser cutter head 350 mm/s showed a better test result of 16 000 rubs. This is almost half of the test result of the abrasion resistance of the untreated denim fabric abrasion resistance tests showed that the lowest power had a minor effect on the fabric's resistance to abrasion. The laser power intensity of 16 W decreased the abrasion resistance of the fabric by about 50 % and the laser power intensity of 18 W burned the fabric intensively, and it is unsuitable for further use. The fabric laser treated at 18 W and the speed of 230 mm/s yarn damages after the abrasion test are shown in Fig. 3. Although the speed of the laser cutter head has a lower effect on a fabric's abrasion properties than power, still slower speed decreased a fabric's abrasion resistance. Laser treated fabrics with the power of 16 W speed decreased fabrics' abrasion resistance between the highest and lowest speed by 44 %.

Fabrics laser treated with the power of 18 W speed decreased their abrasion resistance by 15 000 rubs. The difference between the highest and lowest speed was 94 %.

Abrasion tests showed that the power of 14 W has the smallest effect on the reduction of abrasion resistance. Also, the speed of the laser cutter head 350 mm/s and the power 16 W gave the same optimum strength and appearance to the fabric.

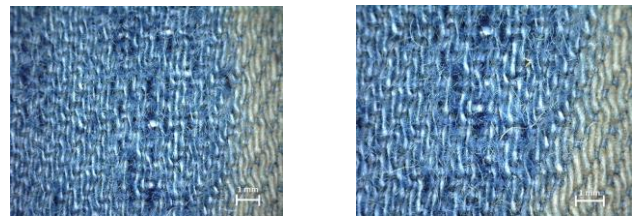


Fig. 3. Fabric laser treated 18 W and 230 mm/s yarn damages after the abrasion test

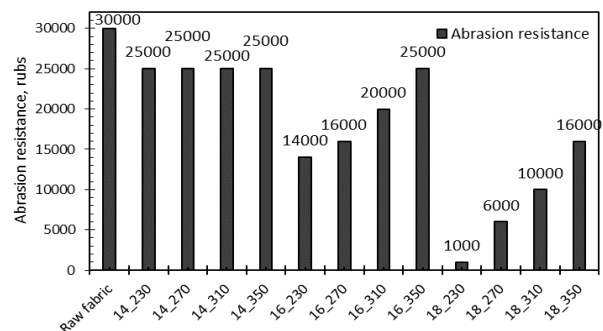


Fig. 4. Comparison of the abrasion test results of laser faded denim fabrics

3.3. Colour measurements

First, the results were obtained ANN described in section 2.3.1. In the case of the colour difference model, the configuration $L = 1$, $N_{in} = 2$, and $N_{tr} = 20$, was used, which results in $N_h = 6$. The Levenberg–Marquardt algorithm and commonly used value of the learning rate $lr = 0.05$ were utilized for error backpropagation [31]. Using the ANN model developed, the response surface for the colour

difference was composed (Fig. 5). In Fig. 5 and below the term “laser speed” is used as an abbreviation for the speed of the laser cutter head. The mean square error is depicted in Fig. 6.

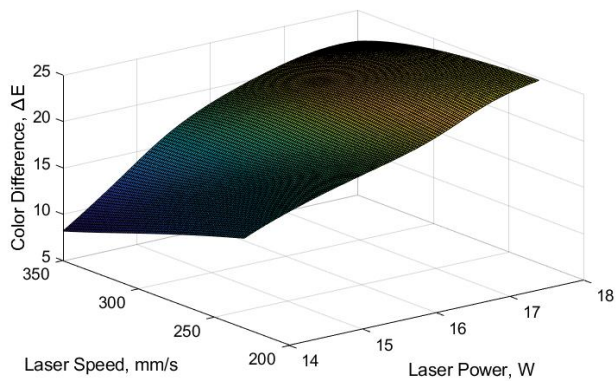


Fig. 5. Response surface for colour difference (101 × 101 points)

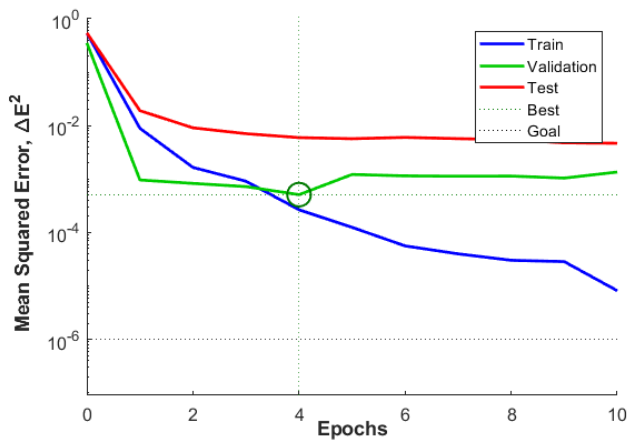


Fig. 6. Mean Squared error of the ANN model for colour difference

In Fig. 5, the values of the design variables and colour difference function are given in terms of original values to get a more realistic picture. Actually, in the model development, both the design variables and the function are used in normalized form.

The response surface of colour differences, using the HWM model described in section 2.3.2, is given in Fig. 7.

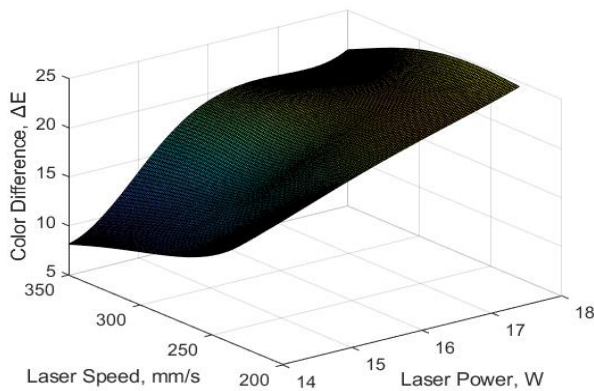


Fig. 7. Response surface of colour differences

Fig. 7 shows that the colour difference of laser treated fabrics was higher when using a lower speed of the laser cutter head and higher power. The highest colour difference

value was shown by fabric laser treated 18 W and 230 mm/s ($\Delta E = 24.48 \pm 0.35$) and fabric laser treated 18 W and 270 mm/s ($\Delta E = 24.72 \pm 0.55$). The lowest colour difference was shown by the laser treated denim fabric with the power of 14 W and a speed of 350 mm/s ($\Delta E = 8.14 \pm 0.47$). The test result is three times better as compared to the highest colour difference (Fig. 8).

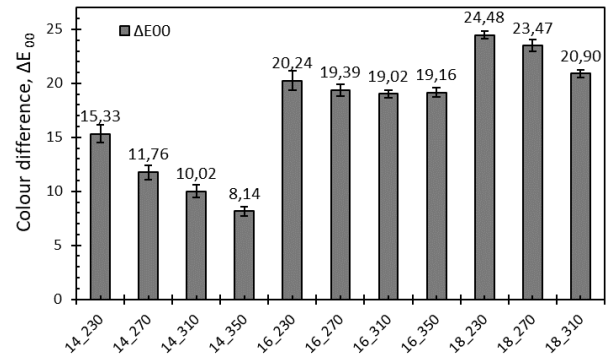


Fig. 8. Comparison of colour difference of laser faded denim fabrics

3.4. Multicriteria design optimization

The multicriteria optimization problem is formulated in section 2. The strategy proposed in section 2 is based on utilizing the weighted summation technique for non-conflicting objectives and the Pareto concept for conflicting objectives.

In the current study, the tear force is considered two times more important than the weft strength, i.e., $w_1 = 2/3$ and $w_2 = 1/3$. The Pareto concept is applied to the combined strength and colour difference criteria (Fig. 9).

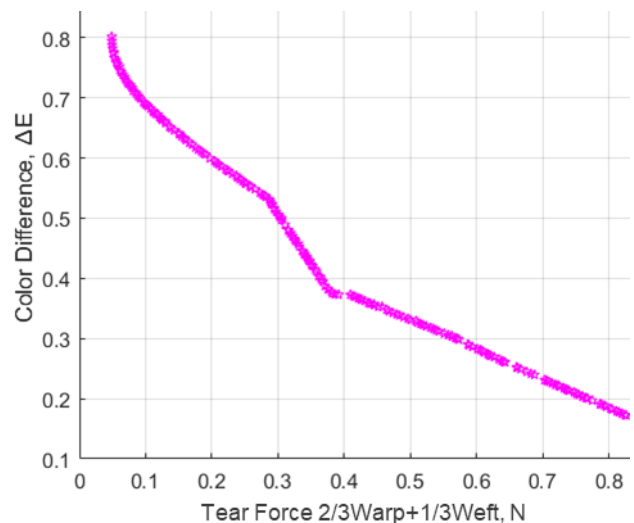


Fig. 9. Combined strength vs. colour difference criteria

Since the objectives are normalized, the smaller value in the Pareto front is better for both criteria with a non-reachable ideal point in (0,0). Near linear behaviour of the compared criteria can be observed from Fig. 9. Any point in the Pareto front is an optimal solution, but the selection of the final solution is not simple in the case of a nearly linear curve since the improvement of strength leads to a decrease of the colour difference in the same range. A separate Pareto front was composed for abrasion resistance and the colour

difference criteria, which are contradictory (Fig. 10).

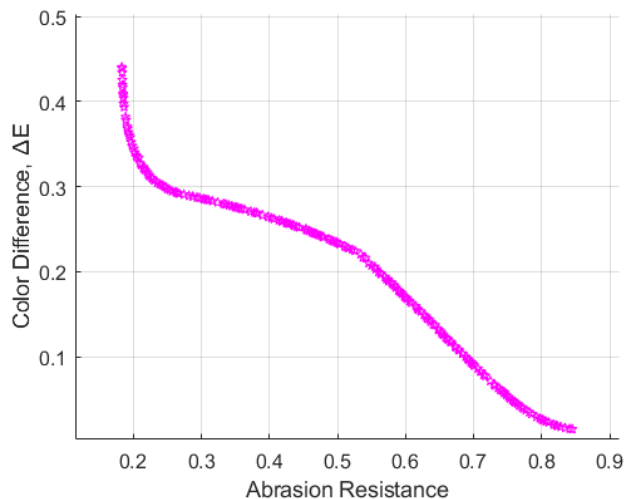


Fig. 10. Abrasion resistance vs. colour difference criteria

The latter Pareto curve is strongly nonlinear and includes rapid growth, i.e., it is suitable for the selection of the final solution. In the current study, the final optimal solution for the whole optimization problem is selected from Fig. 10, since the relation of strength versus colour difference relation does not give clear preferences (near linear behaviour). The detailed values of the design variables, objective functions, etc. are given in the results section. Alternatively, the simplest approach available for solving the posed MDO problem is to combine all three non-conflicting mechanical criteria into one by use of the weighted summation technique and then apply the Pareto concept to the combined and colour difference criteria. This approach is not used in the current study since combining strength criteria with abrasion resistance leads to the loss of direct practical meaning of this combined criterion. As a result, it is complicated to select the final optimal solution in the Pareto front. Additionally, specifying the weights for combining two strength and abrasion resistance criteria is not straightforward.

Due to different datasets available for strength and abrasion resistance criteria (strength measurements failed for fabrics that were treated with the laser power of 18 W), the strength and abrasion resistance criteria were not combined. These criteria have also different meaning. Two Pareto fronts were composed (depicted in Fig. 9 and Fig. 10). First, for the combined strength and colour difference criteria and second, for the abrasion resistance and colour difference criteria. The first Pareto front does not provide a clear preference for the selection final optimal solution since near linear behaviour was observed between the combined strength and the colour difference criteria (Fig. 9). Multicriteria optimization is performed by combining multicriteria genetic algorithm with ANN and HOHWM models. The final optimal solution was determined from the Pareto front given in Fig. 10 as a point before the rapid growth of the colour difference function. Based on the non-dimensional values of the objective functions in the selected point on the Pareto front, the original values of the laser treating parameters and objectives functions can be calculated (determined from normalization Eq. 4 and Eq. 5). The rounded values

obtained are: laser power 16 W; the speed of the laser cutter head 350 mm/s; colour difference 20; abrasion resistance 24016 rubs; tear force in the warp direction 51 N; tear force in the weft direction 23 N. These results were obtained on the limited experimental data currently available.

4. CONCLUSIONS

Multicomponent denim fabric was laser treated at different laser beam power and the speed of the laser cutter head to assess the influence of laser treatment on the fabric strength and appearance properties. Tested fabric warp yarn was made of cotton fibre, weft yarn contained elastane, viscose, and polyester at the core; cotton was used as the sheath fibre. Based on the test results, the mathematical models for four optimality criteria were developed. The multicriteria design optimization problem was formulated and solved by combining the weighted summation technique and the Pareto concept, also multicriteria genetic algorithms.

According to the physico-mechanical tests and mathematical modelling two combinations of optimum laser treating parameters were determined that provided optimum durability properties. The speed of the laser cutter head of 350 mm/s with the laser power of 16 W. Also, the combination of the speed 230 mm/s with the power 14 W.

Novelty of the current study is mainly related with HOHWM based model development. The HOHWM was introduced by workgroup for solving differential equations in 2018 and for function approximation in 2020 [33].

Acknowledgments

The authors are grateful for cooperation with Kipaş Holding A.Ş. for the production of the fabric sample. We also express gratitude to Pöldma Kaubanduse Ltd for their contribution and financial assistance for the study. The study was supported by the Estonian Centre of Excellence in Zero Energy and Resource Efficient Smart Buildings and Districts, ZEBE, TK146 funded by the European Regional Development Fund (grant 2014-2020.4.01.15-0016).

REFERENCES

1. Said, S., Feki, I., Halaoua, S., Hamdaoui, M., Sahraoui, W. The Effect of Ecological Washing Treatments on the Comfort Properties of Dyed Cotton Fabrics *Alexandria Engineering Journal* 61 (12) 2022: pp. 11091–11098. <https://doi.org/10.1016/j.aej.2022.04.045>
2. Mathews, K. *Encyclopedic Dictionary of Textile Terms*. Vol. 2. Woodhead Publishing, New Delhi, 2018.
3. Nayak, R., Padhye, R. *Garment Manufacturing Technology*. Woodhead Publishing, Cambridge, 2015: pp. 396–396.
4. Belzagui, F., Gutiérrez-Bouzán, C. Review on Alternatives for the Reduction of Textile Microfibers Emission to Water *Journal of Environmental Management* 317:115347 2022: pp. 1–12. <https://doi.org/10.1016/j.jenvman.2022.115347>
5. Rahman, O. Understanding Consumers' Perceptions and Behaviour: Implications for Denim Jeans Design *Journal of Textile and Apparel Technology and Management* 7 (1) 2011: pp. 1–16.

6. **Ondogana, Z., Pamuk, O., Ondogan, E.N., Ozguney, A.** Improving the Appearance of All Textile Products from Clothing to Home Textile Using Laser Technology *Optics & Laser Technology* 37 2005: pp. 631–637.
<https://doi.org/10.1016/j.optlastec.2004.10.001>
7. **Abbott, A., Ellison, M.** Biologically Inspired Textiles, Woodhead Publishing, Boca Raton, 2008: pp. 128–129.
8. **Claxton, S., Cooper, T., Hill, H., Holbrook, K.** Opportunities and Challenges of New Product Development and Testing for Longevity in Clothing *PLATE conference paper*, Nottingham Trent University, 17–19 June 2015.
9. **Muthu, S.S., Gardetti, M.Á.** Sustainability in the Textile and Apparel Industries Sustainable Textiles. Clothing Design and Repurposing, 1st Ed., Springer, Gewerbestrasse, 2020: pp. 265–266.
10. **Gandhi, K.** Woven Textiles - Principles, Technologies and Applications, 2nd Ed., Woodhead Publishing, Duxford, 2020: p. 439.
11. **Angelova, Y., Lazov, L., Mezinska, S.** Innovative Laser Technology in Textile Industry Marking and Engraving *Environment Technology Resources Proceedings of the International Scientific and Practical Conference* 3 2017: pp. 15–21.
12. **Vilumsone-Neme, I.** Industrial Cutting of Textile Materials, 2nd Ed., Woodhead Publishing, Duxford, 2018: pp. 168–169.
13. **Juciene, M., Urbelis, V.V., Juchneviene, Ž., Saceviciene, V., Dobilaitė, V.** The influence of Laser Treatment and Industrial Washing on Denim Fabric Tension Properties *International Journal of Clothing Science and Technology* 30 (4) 2018: pp. 588–596.
<https://doi.org/10.1108/IJCST-03-2017-0032>
14. **Kan, C.W.** CO₂ Laser Treatment as a Clean Process for Treating Denim Fabric *Journal of Cleaner Production* 66 2014: pp. 624–63.
<https://doi.org/10.1016/j.jclepro.2013.11.054>
15. **Ozguney, A.T., Özçelik, G., Özkaya, K.** A Study on Specifying the Effect of Laser Fading Process on the Colour and Mechanical Properties of the Denim Fabrics *Tekst Konfeksiyon* 19 (2) 2009: pp. 133–138.
16. **Dalbaşia, E.S., Kayserib, G.Ö., İlleezb, A.A.** A Research on the Effect of Various Laser Fading Parameters on Physical and Surface Properties of Denim Fabric *Optics & Laser Technology* 118 2019: pp. 28–36.
<https://doi.org/10.1016/j.optlastec.2019.04.030>
17. **Solaiman Saha, J.** Comparative Analysis of Manual Fading and Laser Fading Process on Denim Fabric *Science Discovery* 3 (6) 2015: pp. 44–49.
<https://doi.org/10.13140/RG.2.1.1285.6807>
18. **Hutten, I.M.** Handbook of Nonwoven Filter Media, 2nd Ed., Elsevier, Oxford, 2016: p. 374.
19. **Menghe, M., Xin, J.H.** Engineering of High-Performance Textiles. Woodhead Publishing, Duxford, 2017: pp. 69–73.
20. **Rouette, H.K.** Encyclopedia of Textile Finishing. Springer, Aachen, 2001: p. 30.
21. **Chen, C.F., Hsiao, C.H.** Haar Wavelet Method for Solving Lumped and Distributed-Parameter Systems *IEE Proceedings, Control Theory and Applications* 144 (1) 1997: pp. 87–94.
<https://doi.org/10.1049/ip-cta:19970702>
22. **Lepik, Ü., Hein, H.** Haar Wavelets: with Applications. Springer, Cham, 2014: p. 207.
23. **Xie, X.Z., Guoyong, J., Wanyou, L., Zhigang, L.** A Numerical Solution for Vibration Analysis of Composite Laminated Conical, Cylindrical Shell and Annular Plate Structures *Composite Structures* 111 2014: pp. 20–30.
<https://doi.org/10.1016/j.compstruct.2013.12.019>
24. **Wang, L., Ma, Y., Meng, Z.** Haar Wavelet Method for Solving Fractional Partial Differential Equations Numerically *Applied Mathematics and Computation* 227 (2) 2014: pp. 66–76.
<https://doi.org/10.1016/j.amc.2013.11.004>
25. **Islam, S.U., Aziz, I., Al-Fhaid.** An Improved Method Based on Haar Wavelets for Numerical Solution of Nonlinear Integral and Integro-Differential Equations of First and Higher Orders *Journal of Computational and Applied Mathematics* 260 2014: pp. 449–469.
<https://doi.org/10.1016/j.cam.2013.10.024>
26. **Majak, J., Pohlak, M., Karjust, K., Eerme, M., Kurnitski, J., Shvartsman, B.S.** New Higher Order Haar Wavelet Method: Application to FGM Structures *Composite Structures* 201 2018: pp. 72–78.
27. **Sorrenti, M., Di Sciuva, M., Majak, J., Auriemma, F.** Static Response and Buckling Loads of Multilayered Composite Beams Using the Refined Zigzag Theory and Higher-order Haar Wavelet Method *Mechanics of Composite Materials* 57 (1) 2021: pp. 1–18.
<https://doi.org/10.1007/s11029-021-09929-2>
28. **Ratas, M., Salupere, A., Majak, J.** Solving Nonlinear PDEs Using the Higher Order Haar Wavelet Method on Nonuniform and Adaptive Grids *Mathematical Modelling and Analysis* 26 (1) 2021: pp. 147–169.
<https://doi.org/10.3846/mma.2021.12920>
29. **Ratas, M., Majak, J., Salupere, A.** Solving Nonlinear Boundary Value Problems Using the Higher Order Haar Wavelet Method *Journal of Mathematics* 9 (21) 2021: pp. 2809.
<https://doi.org/10.3390/math9212809>
30. **Majak, J., Shvartsman, B., Ratas, M., Bassir, D., Pohlak, M., Karjust, K., Eerme, M.** Higher-order Haar Wavelet Method for Vibration Analysis of Nanobeams *Materials Today Communications* 25 2021: pp. 101290.
<https://doi.org/10.1016/j.mtcomm.2020.101290>
31. **Jena, S.K., Chakraverty, S., Mahesh, V., Harursampath, D.** Wavelet-Based Techniques for Hygro-Magneto-Thermo Vibration of Nonlocal Strain Gradient Nanobeam Resting on Winkler-Pasternak Elastic Foundation *Engineering Analysis with Boundary Elements* 140 2022: pp. 494–506.
<https://doi.org/10.1016/j.enganabound.2022.04.037>
32. **Bulut, F., Oruç, Ö., Esen, A.** Higher Order Haar Wavelet Method Integrated with Strang Splitting for Solving Regularized Long Wave Equation *Mathematics and Computers in Simulation* 197 2022: pp. 277–290.
<https://doi.org/10.1016/j.matcom.2022.02.006>
33. **Majak, J., Eerme, M., Haavajõe, A., Karunanidhi, R., Scholz, D., Lepik, A.** Function Approximation Using Haar Wavelets *AIP Conference Proceedings* 229324 2020: pp. 230004.
<https://doi.org/10.1063/5.0026543>
34. **Majak, J., Mikola, M., Pohlak, M., Eerme, M., Karunanidhi, R.** Modelling FGM materials. An Accurate Function Approximation Algorithms *Proceedings of the International Conference of DAAAM Baltic* 012013 2021: pp. 182815.
<https://doi.org/10.1088/1757-899X/1140/1/012013>
35. **Maynard, M.** Neural Networks: Introduction to Artificial Neurons, Backpropagation and Multilayer Feedforward

Neural Networks with Real-World Applications. Independently published, Michigan 2 2020: p. 53.

36. **Vlachas, P.R., Pathak, J., Hunt, B.R., Sapsis, T.P., Girvan, M., Ott, E., Koumoutsakos, P.** Backpropagation Algorithms and Reservoir Computing in Recurrent Neural Networks for the Forecasting of Complex Spatiotemporal Dynamics *Neural Networks* 126 2020: pp. 191–217. <https://doi.org/10.1016/j.neunet.2020.02.016>
37. **Gnana, K., Sheela Deepa, S.N.** Review of Methods to Fix Number of Hidden Neurons in Neural Networks *Mathematical Problems in Engineering* 2013: pp. 1–11. <https://doi.org/10.1155/2013/425740>
38. **Herranen, H., Majak, J., Tsukrejev, P., Karjust, K., Märtens, O.** Design and Manufacturing of Composite Laminates with Structural Health Monitoring Capabilities *Procedia CIRP* 72 2018: pp. 647–652. <https://doi.org/10.1016/j.procir.2018.03.128>
39. **Majak, J., Pohlak, M., Eerme, M., Velsker, T.** Design of Car Frontal Protection System Using Neural Networks and Genetic Algorithm *Mechanica* 18 (4) 2012: pp. 453–460. <https://doi.org/10.5755/j01.mech.18.4.2325>
40. **Pohlak, M., Majak, J., Karjust, K., Küttner, R.** Multi-criteria Optimization of Large Composite Parts *Composite Structures* 92 (9) 2010: pp. 2146–2152. <https://doi.org/10.1016/j.compstruct.2009.09.039>
41. **Aruñit, A., Kers, J., Goljandin, D., Saarna, M., Tall, K., Majak, J., Herranen, H.** Particulate Filled Composite Plastic Materials from Recycled Glass Fibre Reinforced Plastics *Materials Science (Medžiagotyra)* 17 2011: pp. 1–6. <https://doi.org/10.5755/j01.ms.17.3.593>
42. **Sourabh, K., Sumit, C., Vijay, K.** A Review on Genetic Algorithm: Past, Present, and Future *Multimedia Tools and Applications* 80 2021: pp. 8091–8126. <https://doi.org/10.1007/s11042-020-10139-6>
43. **Deb, K., Pratap, A., Agarwal, S., Meyarivan, T.** A Fast and Elitist Multiobjective Genetic Algorithm: NSGA-II *IEEE Transactions on Evolutionary Computation* 6 (2) 2002: pp. 182–197. <https://doi.org/10.1109/4235.996017>
44. **Jaanuska, L., Hein, H.** Delamination Quantification by Haar Wavelets and Machine Learning *Mechanics of Composite Materials* 58 (2) 2022: pp. 249–260. <https://doi.org/10.1007/s11029-022-10025-2>
45. **Aydin, L., Artem, H.S., Deveci, H.A.** Single- and Multiobjective Optimizations of Dimensionally Stable Composites Using Genetic Algorithms *Mechanics of Composite Materials* 57 (3) 2021: pp. 321–336. <https://doi.org/10.1007/s11029-021-09957-y>
46. **Barkanov, E., Akishin, P., Namsone, E., Auzins, J., Morozovs, A.** Optimization of Pultrusion Processes for an Industrial Application *Mechanics of Composite Materials* 56 (6) 2021: pp. 697–712. <https://doi.org/10.1007/s11029-021-09916-7>
47. **Janeliukstis, R., Mironovs, D.** Smart Composite Structures with Embedded Sensors for Load and Damage Monitoring – A Review *Mechanics of Composite Materials* 57 (2) 2021: pp. 131–152. <https://doi.org/10.1007/s11029-021-09941-6>
48. **Majak, J., Pohlak, M.** Decomposition Method for Solving Optimal Material Orientation Problems *Composite Structures* 92 (8) 2010: pp. 1839–1845.
49. **ISO 12947-2:2016.** Textiles - Determination of the Abrasion Resistance of Fabrics by the Martindale Method – Part 2: Determination of Specimen Breakdown.
50. **ISO 13937-2:2000.** Textiles. Tear Properties of Fabric. Part 2: Determination of Tear Force of Trouser-Shaped Specimens (Single Tear Method).
51. **Konica Minolta Sensing.** Precise Color Communication. Booklet, Japan, 2007: pp. 56–57.
52. **Mustafidah, H., Putri, C.P., Harjono, H., Suwarsito, S.** The Most Optimal Performance of The Levenberg-Marquardt Algorithm Based on Neurons in the Hidden Layer *Journal of Physics: Conference Series* 1402 (066099) 2019: pp. 1–16. <https://doi.org/10.1088/1742-6596/1402/6/066099>



© Mandre et al. 2023 Open Access This article is distributed under the terms of the Creative Commons Attribution 4.0 International License (<http://creativecommons.org/licenses/by/4.0/>), which permits unrestricted use, distribution, and reproduction in any medium, provided you give appropriate credit to the original author(s) and the source, provide a link to the Creative Commons license, and indicate if changes were made.